Thermodynamic modelling assessment of the ternary system Cs-Mo-O

Smith, A. L.; Pham Thi, T. N.; Guéneau, C.; Dumas, J. C.; Epifano, E.; van Burik, W.; Dupin, N.

DOI
10.1016/j.calphad.2021.102350

Publication date
2021

Document Version
Final published version

Published in
Calphad: Computer Coupling of Phase Diagrams and Thermochemistry

CALPHAD: Computer Coupling of Phase Diagrams and Thermochemistry 75 (2021) 102350

Contents lists available at ScienceDirect

Calphad

journal homepage: www.elsevier.com/locate/calphad

Thermodynamic modelling assessment of the ternary system Cs-Mo-O

A.L. Smith [a,*], T.N. Pham Thi [b], C. Guéneau [c], J.-C. Dumas [b], E. Epifano [a,e], W. van Burik [a], N. Dupin [d]

[a] Delft University of Technology, Faculty of Applied Sciences, Radiation Science & Technology Department, Mekelweg 15 2629 JB Delft, The Netherlands
[b] CEA, DES, IRESNE, DEC, Cadarache F-13108 Saint-Paul-Lez-Durance, France
[c] Université Paris-Saclay, CEA, Service de la Corrosion et du Comportement des Matériaux dans leur Environnement, 91191, Gif-sur-Yvette, France
[d] Calcul Thermodynamique, 3 rue de l'avenir, 63670 Orcet, France
[e] CIRIMAT laboratory, University of Toulouse, CNRS, INPT, UPS, ENSIACET 4 allée Emile Monso, BP-44362, 31030 Toulouse Cedex 4, France

ARTICLE INFO

Keywords:
Joint oxyde-gaine
Cesium polymolybdates
CALPHAD
Fast neutron reactors

ABSTRACT

This work reports the thermodynamic modelling assessment of the rather complex Cs-Mo-O system, which is key for the understanding of fission products chemistry in oxide fuelled Light Water Reactors (LWRs) and next generation Sodium-cooled and Lead-cooled Fast Reactors (SFRs and LFRs). The model accounts for the existence of the ternary molybdates Cs_2MoO_4 (α and β), $Cs_2Mo_2O_7$ (α and β), $Cs_2Mo_3O_{10}$, $Cs_2Mo_4O_{13}$, $Cs_2Mo_5O_{16}$, and $Cs_2Mo_7O_{22}$, for which sufficient structural and thermodynamic information are available in the literature. These phases are treated as stoichiometric in the model. The liquid phase is described with an ionic two-sublattice model, and the gas phase as an ideal mixture. The optimized Gibbs energies are assessed with respect to the known thermodynamic and phase equilibrium data in the Cs_2MoO_4-MoO_3 pseudo-binary section. A good agreement is generally obtained within experimental uncertainties. The calculated vapour pressures above Cs_2MoO_4 (solid and liquid) are also compared to the available experimental data. Finally, isotherms of the Cs-Mo-O ternary phase diagram are calculated at relevant temperatures for the assessment of the fuel pin behaviour in LWRs, SFRs and LFRs.

1. Introduction

The safety assessment of nuclear fuel behaviour in a nuclear fission reactor requires the development of models and simulation codes of the complex chemistry of the numerous fission products generated during irradiation. The chemical elements generated inside the oxide fuel matrix (U, Pu)O_2 of Light Water Reactors (LWRs) and next generation Sodium-cooled and Lead-cooled Fast Reactors (SFRs and LFRs) form gaseous or volatile species, metallic precipitates, oxide precipitates, or constitute soluble species according to the classification of Kleykamp [1]. The exact speciation depends on the specific physico-chemical properties of the elements, and the conditions on burnup (as well as isotopic composition of the fuel and neutron flux spectrum), temperature, and oxygen potential under normal operation and accidental conditions. Among those fission products, the speciation of cesium and molybdenum is of particular interest. Cs and Mo are firstly generated with a high fission yield (e.g. ~20 and 21% in the fast reactor Phénix fuel pin ($U_{0.77}Pu_{0.23}O_{2-x}$) at 10 at. % burnup [2]). Moreover, cesium belongs to the class of volatile products [3], and the potential release of ^{135}Cs and ^{137}Cs to the coolant and subsequently to the environment in a severe accident scenario should be assessed carefully for the protection of the general public.

The chemical form of cesium varies with the value of the oxygen potential that increases during irradiation. For low oxygen potential values, e.g. around − 500 kJ·mol^{-1} in hypostoichiometric oxide fuels, the formation of CsI, Cs_2Te, Cs_2UO_4 and Cs_2MoO_4 is expected from thermodynamic calculations in increasing order of abundance [2]. For higher oxygen potential values, e.g. above − 400 kJ·mol^{-1}, CsI and Cs_2MoO_4 become the most stable compounds (again in this increasing order of abundance as the yield of iodine, ~ 9%, is much lower than that of molybdenum) [2]. The formation of Cs_2MoO_4 is thus expected to be rather significant, especially at high burnups, as is the case in fast neutron reactors such as in SFRs and LFRs.

A phenomenon very specific to fast reactor oxide fuel pin is in fact observed at the (U, Pu)O_2 fuel periphery, namely the formation of a so-called JOG (*Joint-Oxyde-Gaine*, a French term that corresponds to the oxide-cladding joint) layer, at high burn-up (above 7%–8% fission per initial metal atom), in between fuel and cladding. The volatile fission products mentioned earlier (Cs but also I, Te, Mo) migrate radially due to the high thermal gradients in this type of fuel (~973 K at the

* Corresponding author.
E-mail address: a.l.smith@tudelft.nl (A.L. Smith).

https://doi.org/10.1016/j.calphad.2021.102350
Received 13 July 2021; Received in revised form 20 August 2021; Accepted 2 September 2021
Available online 1 October 2021

periphery and ~2273 K at the centre), and build up in the cooler rim region in the JOG layer of thickness 150–300 μm [2].

The JOG layer was found to have a porous and highly heterogeneous structure, and was reported to include the fission products (Cs, Mo, Te, I, Zr, Ba) and cladding components (Fe, Cr) [4]. From the combination of post-irradiation examinations (PIE) and thermodynamic calculations, the JOG layer was shown to be made of Cs_2MoO_4 (main constituent), CsI, Cs_2Te and Cs_2UO_4 [4–10]. The presence of higher polymolybdates was also reported in localized areas by Cappia et al. [4], in particular $Cs_2Mo_3O_{10}$. The authors also reported the signature of a structure with monoclinic $P2_1/c$ symmetry, which they attributed to $Cs_2Ba_2O_3$ (following Cs decay into Ba), but could also be interpreted as α-$Cs_2Mo_2O_7$. From these findings, it is clear that a thorough knowledge of the thermochemistry of the Cs–Mo–O system, and of the thermochemical and thermophysical properties of its constituting cesium polymolybdates is essential for the assessment of the fuel behaviour. It is in particular worth mentioning that Cs_2MoO_4 has a thermal conductivity lower than the fuel by about one order of magnitude [11,12]. It also shows a strong and anisotropic thermal expansion upon increasing temperature at the expected operating temperatures [13]. All these data are necessary to feed so-called Fuel Performance Codes (FPCs) that are able to predict fuel pin behaviour at the engineering scale.

This work reports a thermodynamic modelling assessment of the key Cs–Mo–O system, based on the CALPHAD methodology, and with descriptions compatible with the formalisms used in the TAF-ID database (Thermodynamics of Advanced Fuels – International Database) of the OECD/NEA [14]. The available literature data, including structural, thermodynamic, phase diagram and vapour pressure data, are first critically reviewed, after which the models used are described in detail, and benchmarked against the experimental information.

2. Review of literature data

Cs–Mo–O is a rather complex system, with a number of ternary cesium molybdate phases reported: Cs_2MoO_4, $Cs_2Mo_2O_7$, $Cs_2Mo_3O_{10}$, $Cs_2Mo_4O_{13}$, $Cs_2Mo_5O_{16}$, $Cs_2Mo_7O_{22}$, $Cs_6Mo_2O_9$, $Cs_{0.14}MoO_3$, $Cs_{0.25}MoO_3$, $Cs_{0.33}MoO_3$, $Cs_{0.28}MoO_3$, and $CsMo_{4-x}O_{12}$ ($x = 0.13$) [15]. A comprehensive literature review of this system has been reported by Fabrichnaya [16] and more recently by Smith et al. [17]. Its key features are detailed hereafter, including reported phase diagram data, thermodynamic and vapour pressure data. The thermodynamic assessment reported herein accounts for the following ternary phases, for which sufficient structural and thermodynamic information is available: Cs_2MoO_4 (α and β), $Cs_2Mo_2O_7$ (α and β), $Cs_2Mo_3O_{10}$, $Cs_2Mo_4O_{13}$, $Cs_2Mo_5O_{16}$, and $Cs_2Mo_7O_{22}$. The knowledge on the other phases is too limited to this date to include them in the thermodynamic model.

2.1. Constituting binary systems

The phase diagrams of the three binary sub-systems constituting this ternary system are shown in Figs. 1(a)–1(c). They are already included in the TAF-ID database of the OECD/NEA [14], and were used herein without further modification. The Cs–O system shows eight stable binary oxides Cs_7O, Cs_4O, Cs_7O_2, Cs_3O, Cs_2O, CsO, CsO_2 and CsO_3, all considered stoichiometric in the TAF-ID. The optimized parameters of the corresponding model can be found in Guéneau et al. [18]. The Mo–O system shows five stable binary oxide compounds MoO_2, MoO_3, Mo_4O_{11}, Mo_8O_{23}, Mo_9O_{26}, also treated as stoichiometric. The corresponding model was optimized by Corcoran et al. [19], and the liquid phase parameters were re-assessed by Kauric [20] so as to suppress the appearance of a miscibility gap towards high MoO_3 content in several ternary systems such as Na–Mo–O and Ba–Mo–O [21]. The full list of optimized parameters are given in [21]. The Cs–Mo system is characterized by a low reciprocal solubility of the elements. The available experimental data are scarce. The model for this binary system was optimized in the framework of the Fuelbase project (2011) [22]. The assessed parameters are listed in Appendix.

2.2. Structural data

The crystal structures of the aforementioned ternary phases is summarized in Table 1. Note that two polymorphs have been reported for the Cs_2MoO_4 and $Cs_2Mo_2O_7$ intermediates, with transition temperatures at $T_{tr}(Cs_2MoO_4, \alpha–\beta) = (841.3 \pm 1.0)$ K [23] and $T_{tr}(Cs_2Mo_2O_7, \alpha–\beta) = (650 \pm 5)$ K [17], respectively. Two structures have also been reported for $Cs_2Mo_4O_{13}$, one triclinic, in space group $P-1$ (supposedly the phase stable at room temperature) [24], and one monoclinic, in space group $C2/c$ (supposedly a phase stable at high temperatures). However, the exact transition temperature and nature of the transition between these two modifications is not known with certainty. The phase diagram studies of Hoekstra [25] and Spitsyn and Kuleshov [26], discussed in the next section, suggested the existence of a metastable phase, formed when quenching the melt at room temperature. The authors observed exothermic events in their thermal analysis measurements around 608 K and 643 K, respectively, which Hoekstra interpreted as the transformation from the metastable form to the stable phase of $Cs_2Mo_4O_{13}$ upon heating. The polymorphism of $Cs_2Mo_4O_{13}$ thus still needs to be clarified. We have included only one modification in the present thermodynamic model.

2.3. Phase diagram data

A number of phase equilibria studies have been reported in the pseudo-binary section between Cs_2MoO_4 and MoO_3: by Spitsyn and Kuleshov[1] [26], Salmon and Caillet[2] [29], Hoekstra[3] [25], and Bazarova et al.[4] [30]. Some discrepancies exist between those studies, however. According to the review of Fabrichnaya in 2007 [16], the data of Hoekstra [25] are believed to be most reliable. Smith et al. [17] very recently re-investigated the Cs_2MoO_4–MoO_3 pseudo-binary phase diagram using Differential Scanning Calorimetry (DSC) and coupled Thermogravimetry-Differential Scanning Calorimetry (TG-DSC) to solve some of these discrepancies. The most important outcomes are summarized below:

- the existence of a phase transition in the $Cs_2Mo_2O_7$ compound was confirmed, and measured at $T_{tr} = (650 \pm 5)$ K.
- the melting temperature of $Cs_2Mo_2O_7$ was measured at $T_{fus} = (725 \pm 5)$ K, in good agreement with the data reported previously by Smith et al. [27] (720.2 ± 5.0 K). It should be noted that the other sources report higher values: 737 K for Hoekstra [25], 749 K for Salmon and Caillet [29], and 767 K for Spitsyn and Kuleshov [26].
- the (congruent) melting temperature of $Cs_2Mo_3O_{10}$ was found at $T_{fus} = (806 \pm 5)$ K, which is ~15 K lower than reported by Hoekstra [25] (820 K), Salmon and Caillet [29] (823 K), and Spitsyn and Kuleshov [26] (818 K). It should be noted that the onset temperature of the heat flow curve was selected for the analysis. The extremum temperature of the same heat flow signal yielded (825 ± 5) K, in closer agreement with the other data.
- the peritectic decomposition of $Cs_2Mo_5O_{16}$ was found at $T_{fus} = (813 \pm 5)$ K. Hoekstra, Spitsyn and Kuleshov, and Salmon and Caillet reported 823 K, 823 K and 818 K, respectively.
- the peritectic decomposition of $Cs_2Mo_7O_{22}$ was found at $T_{fus} = (836 \pm 5)$ K, in good agreement with Salmon and Caillet (837 K), but again lower than the data of Hoekstra (846 K). It should be noted that in the work of Salmon and Caillet the latter data point was interpreted as the polymorphic transition of a solid solution around the $Cs_2Mo_9O_{28}$ composition, however.

[1] Thermal analysis by a visual-polythermal technique.

[2] Solid state reactions coupled with X-ray diffraction, Differential Thermal Analysis and infrared spectroscopy.

[3] X-ray diffraction analyses, simultaneous Differential Thermal Analysis-Thermogravimetry Analysis, infrared and Raman spectroscopy.

[4] X-ray diffraction, Differential Thermal Analysis, infrared spectroscopy and electric conductivity measurements.

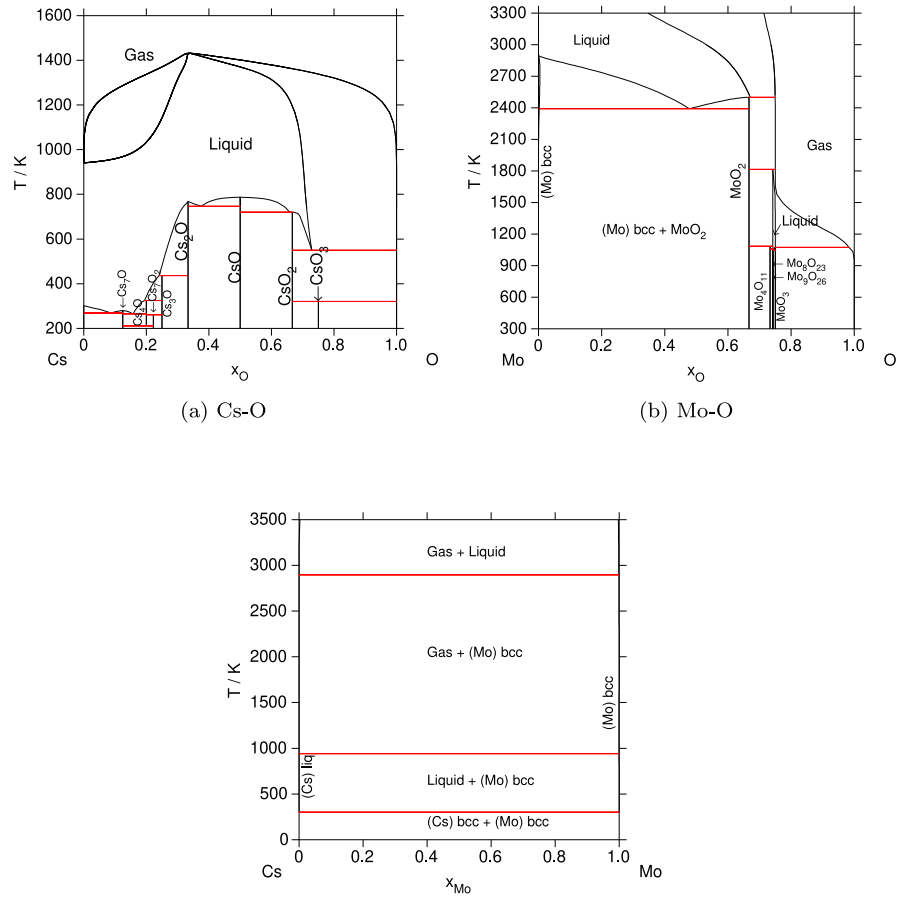

Fig. 1. Phase diagrams of the (a) Cs–O (b) Mo–O and (c) Cs–Mo sub-systems calculated using the TAF-ID models [14].

Table 1
Structural data for the ternary phases in the Cs–Mo–O system (1 Å = 0.1 nm). Uncertainties relative to the last digits are given in parenthesis.

Phase	Symmetry	Space group	Lattice parameters				Ref.
			a/nm	b/nm	c/nm	β/°	
α-Cs_2MoO_4	Orthorhombic	*Pnma*	1.15623(8)	0.65406(4)	0.84906(5)	90	[27]
β-Cs_2MoO_4[a]	Hexagonal	$P6_3/mmc$	0.6840(1)	0.6840(1)	0.8977(2)	90	[13]
α-$Cs_2Mo_2O_7$	Monoclinic	$P2_1/c$	1.5560(2)	1.5184(1)	0.72244(7)	90.120(7)	[17]
β-$Cs_2Mo_2O_7$[b]	Orthorhombic	*Pbcm*	0.799136(11)	1.548597(21)	0.724613(11)	90	[27]
$Cs_2Mo_3O_{10}$	Monoclinic	$C2/c$	1.4472(2)	0.8404(1)	0.9464(1)	97.731(6)	[17]
$Cs_2Mo_4O_{13}$	Triclinic	$P-1$	0.8396(5)	0.8655(5)	1.0413(5)	see[c]	[24]
$Cs_2Mo_4O_{13}$	Monoclinic	$C2/c$	4.592(5)	1.0418(3)	0.7923(8)	92.94(5)	[28]
$Cs_2Mo_5O_{16}$	Monoclinic	$C2/c$	2.1444(2)	0.55600(4)	1.4339(1)	122.735(5)	[17]
$Cs_2Mo_7O_{22}$	Monoclinic	$C2/c$	2.1546(1)	0.55385(3)	1.89179(9)	122.744(3)	[17]

[a]Data measured at T = 948 K.
[b]Data measured at T = 683 K.
[c]α = 106.158(5), β = 103.686(5), γ = 109.761(5).

The collected data by Smith et al. [17] are found generally lower than Hoekstra [25]. It is not clear, however, how the thermal analysis data were treated in the work of Hoekstra with respect to temperature calibration and choice of the offset or onset temperature of the signals, as reported by [17]. The most recent phase equilibrium data by Smith et al. [17] have been selected for the re-assessment of the Cs–Mo–O system as the temperature calibration of the DSC and TG-DSC measurements was carefully checked with the measurement of the well-known three phase transitions and melting temperatures of the Na_2MoO_4 compound [17].

2.4. Thermodynamic data

The standard enthalpies of formation of α-Cs_2MoO_4, α-$Cs_2Mo_2O_7$, $Cs_2Mo_3O_{10}$, $Cs_2Mo_5O_{16}$ and $Cs_2Mo_7O_{22}$ were measured by O'Hare and Hoekstra [31,32], Smith et al. [17,33] and Benigni et al. [34]. The latter data are summarized in Table 2. A very good agreement is seen between the various studies.

The enthalpies of formation listed in Table 2 were derived using a thermochemical cycle involving the enthalpy of formation of MoO_3(cr), i.e. $-(745.0 \pm 1.0)$ kJ·mol^{-1} (value selected in the review by Cordfunke and Konings [23]). The reported uncertainty $\pm$ 1 kJ·mol^{-1} is most probably largely underestimated, however, as stressed by [17]. This value

Table 2
Thermodynamic data reported on the cesium polymolybdates.

Compound	$\Delta_f H^o_m$(cr, 298.15 K) (kJ·mol^{-1})	Ref.	$C^o_{p,m}$(cr, 298.15 K) (J·K^{-1}·mol^{-1})	S^o_m(cr, 298.15 K) (J·K^{-1}·mol^{-1})	Ref.
α-Cs_2MoO_4	−(1514.5 ± 1.0)	[23,31]	148.67 ± 0.15	248.35 ± 0.30	[23,35]
	−(1514.69 ± 1.54)	[33]			
	−(1513.56 ± 1.11)	[34]			
α-$Cs_2Mo_2O_7$	−(2302.4 ± 2.1)	[23,32]	211.9 ± 2.1	317.4 ± 4.3	[27]
	−(2301.84 ± 2.37)	[34]			
	−(2301.6 ± 4.7)	[17]			
$Cs_2Mo_3O_{10}$	−(3077.17 ± 3.47)	[34]			
	−(3075.6 ± 6.5)	[17]			
$Cs_2Mo_5O_{16}$	−(4601.7 ± 5.96)	[34]			
$Cs_2Mo_7O_{22}$	−(6087.16 ± 8.79)	[34]			

Table 3
Re-calculated enthalpies of formation of the cesium polymolybdates based on an uncertainty of 1% on the enthalpy of formation of MoO_3(cr) involved in the thermochemical cycles of the solution calorimetry measurements. The values selected for the present assessment are marked in bold.

Compound	$\Delta_f H^o_m$(cr, 298.15 K) (kJ·mol^{-1})	Ref.
α-Cs_2MoO_4	−(1514.5 ± 7.45)	[23,31]
	−(1514.69 ± 7.54)	[27]
	−(1513.56 ± 7.52)	[34]
	−(1514.2 ± 4.3)	Weighted average (this work)
α-$Cs_2Mo_2O_7$	−(2302.4 ± 14.9)	[23,32]
	−(2301.84 ± 15.07)	[34]
	−(2301.6 ± 15.5)	[17]
	−(2302.1 ± 8.8)	Weighted average (this work)
$Cs_2Mo_3O_{10}$	−(3077.17 ± 22.35)	[34]
	−(3075.6 ± 23.1)	[17]
	−(3076.8 ± 16.1)	Weighted average (this work)
$Cs_2Mo_5O_{16}$	**−(4601.7 ± 37.25)**	[34]
$Cs_2Mo_7O_{22}$	**−(6087.16 ± 52.16)**	[34]

was derived from the average of the measurements of Staskiewicz et al. (−744.65 ± 0.40 kJ·mol^{-1}) [36] and Mah (−745.4± 0.5 kJ·mol^{-1}) [37]. However, the latter data were derived from the incomplete combustion of molybdenum and MoO_2 to MoO_3 (it reached only 70%–93%). Even if corrections were made to account for this, we believe that the quoted final uncertainties amounting to less than 0.07% are largely underestimated. The review by Cordfunke and Konings [23] assigning an uncertainty of 0.1% is already more conservative. But in the present work, the uncertainties on the enthalpies of formation have been re-calculated considering an uncertainty of 1% (± 7.45 kJ·mol^{-1}) on the enthalpy of formation of MoO_3, which is believed to be more realistic as reported already in [17]. The newly assessed uncertainties are listed in Table 3. Moreover, the weighted average of the latter values has been calculated for each composition, and is selected for the present thermodynamic assessment.[5]

The standard entropies of α-Cs_2MoO_4 and α-$Cs_2Mo_2O_7$ were obtained from low-temperature heat capacity measurements using adiabatic calorimetry [35] and thermal-relaxation calorimetry [27], respectively. The measured data are listed in Table 2 and selected for the present assessment.

[5] Note that the final averaged result X was calculated as recommended in [38] for independent source of data as a weighted mean using the formula:

$$X = \frac{\sum_i (X_i/\sigma_i^2)}{\sum_i (1/\sigma_i^2)} \quad (1)$$

The uncertainty was calculated using the formula:

$$\sigma_X = \sqrt{\frac{1}{\sum_i (1/\sigma_i^2)}} \quad (2)$$

Fredrickson and Chasanov [39], Konings and Cordfunke [40], and Denielou et al. [41] reported high temperature enthalpy increment measurements for Cs_2MoO_4 in the temperature ranges (845–1191 K), (415–700 K), and (1232–1500 K), respectively. The review of Cordfunke and Konings [23] discards the data of Fredrickson and Chasanov because of discrepancies with the other sets of data. Kohli and Lacom [42] reported heat capacity measurements in the range 300–800 K using differential scanning calorimetry (DSC). The high temperature heat capacity equations selected in the review by Cordfunke and Konings [23] for α-Cs_2MoO_4 (orthorhombic in space group *Pbam*) and β-Cs_2MoO_4 (hexagonal in space group $P6_3/mmc$) are those of Konings and Cordfunke [40]. The data of Denielou et al. [41] were adopted for the liquid phase in [23]. The heat capacity function of Cs_2MoO_4 was optimized as part of this assessment based on the low-temperature heat capacity data of Osborne et al. [35], high temperature heat capacity data of Kohli and Lacom [42], and enthalpy increment data of Konings and Cordfunke [40].

The high temperature heat capacity of $Cs_2Mo_2O_7$ was measured in the range (310–700 K) by Kohli [43] based on DSC measurements and the step method, but found in poor agreement with the low-temperature heat capacity data of Smith et al. [27]. In their work, Smith et al. [27] suggested an estimation of the high-temperature heat capacity by combining their measured low-temperature heat capacity data in the range (248.7–313.2 K) with data estimated above T = 500 K using the Neumann–Kopp approximation applied to the heat capacity functions of Cs_2MoO_4 [23,35] and MoO_3 [23,44]. The latter function was retained for the present assessment of the Cs–Mo–O system. (See Table 4.)

The reported phase transition temperatures for the cesium polymolybdates are summarized in Table 7 together with the optimized values in the present CALPHAD model. The associated transition enthalpies were determined by Konings and Cordfunke [40], Fredrickson and Chasanov [39], Denielou et al. [41], and Smith et al. [17]. They are also listed in Table 7, where they are compared to the optimized values.

2.5. Vapour pressure data

Several studies have been reported on the vaporization and sublimation of Cs_2MoO_4 (see Table 5), i.e. by Johnson [45] (1070.6–1167.2 K), Tangri et al. [46] (1229–1310 K), Cordfunke et al. [47] (1116.8–1190.1 K), Yamawaki et al. [48] (1134.36–1242.16 K), Kazenas et al. [49] (1026–1148 K), and Stolyarova et al. [50] (1030–1198 K), with a rather good agreement between the various studies. The various works agree on a congruent vaporization and sublimation process with the sole formation of Cs_2MoO_4(g) in the gas phase. The reported experimental data are shown in Fig. 6 together with the calculated vapour pressure over Cs_2MoO_4(cr, l) from our thermodynamic model.

Thi-Mai-Dung Do et al. [52] investigated the vaporization of $Cs_2Mo_2O_7$ by combining thermogravimetry with a transpiration method. The authors suggested a congruent vaporization for $Cs_2Mo_2O_7$(l) and

Table 4
Summary of heat capacity data for Cs_2MoO_4.

Phase	$C_{p,m} = A + B\cdot T + C\cdot T^{-2} + D\cdot T^2$/J·K^{-1}·mol^{-1}				Temp. range/K	Ref.
	A	B	C	D		
Cs_2MoO_4(cr, α)	116.404	$108.2212\cdot10^{-3}$			298.15–841.3	[23]
Cs_2MoO_4(cr, β)	122.295	$97.049\cdot10^{-3}$			841.3–1229.5	[23]
Cs_2MoO_4(cr)	95.9182	$18.82224\cdot10^{-2}$	− 95472	$-7.0314\cdot10^{-5}$	298.15–1229.5	This work
Cs_2MoO_4(l)	210.154				>1229.5	[23]
$Cs_2Mo_2O_7$(cr)	266.321	$7.173\cdot10^{-2}$	$-5.65075\cdot10^{6}$		310–700	[43]
$Cs_2Mo_2O_7$(cr)	131.487	0.30519		$-1.12277\cdot10^{-4}$	250–720	[27]

Table 5
Experimental data on the vaporization behaviour of Cs_2MoO_4. KEMS: Knudsen Effusion Mass Spectrometry.

Reference	$\log P_{10}$(Pa)	T(K)	Method	Cell/crucible material
Johnson [45]	(11.58 ± 0.02)–(13984 ± 600)/T(K)[a]	1070.6–1167.2	KEMS	Alumina[c]
Tangri et al. [46]	(9.37 ± 0.29)–(11452 ± 370)/T(K)[b]	1229–1310 K	Transpiration[h]	Alumina
Cordfunke et al. [47]	(12.038 ± 0.507)–(14470.5 ± 584.7)/T(K)[f]	1116.8–1190.1 K	Transpiration[h]	Gold[d]
Cordfunke et al. [47]	(11.850 ± 0.567)–(14229.3 ± 653.6)/T(K)[g]	1116.8–1190.1 K	Transpiration[h]	Gold[d]
Yamawaki et al. [48]	9.80–12100/T(K)	1231.56–1242.16 K	KEMS	Alumina[e]
Yamawaki et al. [48]	11.02–13600/T(K)	1134.36–1206.01 K	KEMS	Alumina[e]
Kazenas et al. [49]	11.47–13724/T(K)	1026–1148 K	KEMS	Platinum
Stolyarova et al. [50]	(11.5 ± 0.9)–(13616 ± 514)/T(K)	1030–1198 K	KEMS (twin-cells)	Platinum

[a]The authors report a 5% uncertainty on the vapour pressures.
[b]The authors report a 10% uncertainty on the vapour pressures.
[c]Molybdenum effusion cell with gold liner and alumina crucible inside the gold liner.
[d]Y_2O_3-stabilized zirconia condenser tube with a protective gold tube.
[e]Molybdenum effusion cell with alumina liner.
[f]Data based on cesium analyses.
[g]Data based on molybdenum analyses.
[h]Dry oxygen carrier gas.

Table 6
Thermodynamic data optimized in this work. *SER* refers to the phase of the element stable at 298.15 K. Optimized coefficients are shown in bold.

Phase	Gibbs energy/(J·mol^{-1})	Ref.
Liquid	${}^{o}G(Cs^+)_2(MoO_4^{2-}) - 2{}^{o}H_{Cs}^{SER} - {}^{o}H_{Mo}^{SER} - 4{}^{o}H_{O}^{SER} = G_{Cs_2MoO_4}$ **+ 36437.799 − 31.504173T**	This work
	$L^0(Cs^+)_P(MoO_4^{2-},MoO_3)_Q$ **= −96000 − 11T**	This work
	$L^1(Cs^+)_P(MoO_4^{2-},MoO_3)_Q$ **= 62000**	This work
	$L^2(Cs^+)_P(MoO_4^{2-},MoO_3)_Q$ **= −9000**	This work
Hexavalent molybdates	$G_{\alpha-Cs_2MoO_4} = G_{Cs_2MoO_4}$	This work
	$G_{\beta-Cs_2MoO_4} = G_{Cs_2MoO_4}$ **+ 4600 − 5.4677T**	This work
	$G_{\alpha-Cs_2Mo_2O_7} = G_{Cs_2Mo_2O_7}$	This work
	$G_{\beta-Cs_2Mo_2O_7} = G_{Cs_2Mo_2O_7}$ **+ 423 − 0.650769T**	This work
	$G_{Cs_2Mo_3O_{10}} = G_{Cs_2MoO_4} + 2G_{MoO_3}$ **−53000 − 12T**	This work
	$G_{Cs_2Mo_4O_{13}} = G_{Cs_2MoO_4} + 3G_{MoO_3}$ **−76017 + 8.9T**	This work
	$G_{Cs_2Mo_5O_{16}} = G_{Cs_2MoO_4} + 4G_{MoO_3}$ **−89000 + 17T**	This work
	$G_{Cs_2Mo_7O_{22}} = G_{Cs_2MoO_4} + 6G_{MoO_3}$ **−103000 + 26.4T**	This work
Gas	${}^{o}G_{Cs_2MoO_4}^{gas} - 2{}^{o}H_{Cs}^{SER} - {}^{o}H_{Mo}^{SER} - 4{}^{o}H_{O}^{SER} = G_{Cs_2MoO_4}^{G}$	This work
functions	$G_{Cs_2MoO_4}$ **= −1554486.3 + 448.47296T − 95.9182T** ln**(T) − 0.0941112T^2 + 1.1719·10^{-5}T^3 + 47736T^{-1}**	This work
	$G_{Cs_2Mo_2O_7}$ **= −2354000 + 651.0**T − 131.487Tln (T) − 0.152595T^2 + 1.87128333·10^{-5}T^3	This work
	$G_{Cs_2MoO_4}^{G}$ = −1246344 + 340.447912T − 110.7356Tln (T) − 0.05133275T^2 + 1.09630117·10^{-5}T^3 +454105.3T^{-1} (298.15–600 K)	[51]
	= −1263115.58 + 612.12144T − 153.3783Tln (T) − 0.002280958T^2 + 2.12845167·10^{-7}T^3 +1714266T^{-1} (600–1700 K)	[51]
	= −1258019.45 + 595.921622T − 151.5654Tln (T) − 0.001915096T^2 + 1.049755·10^{-7}T^3 (1700–6000 K)	[51]

the formation of $Cs_2Mo_2O_7$(g) gaseous species. They derived the following equation for the total vapour pressure in the temperature range (1273–1573 K) based on their thermogravimetry data and the Langmuir equation for free evaporation [53]:

$$\log_{10} P(Pa) = (8.95 \pm 0.07) - (10300 \pm 100)/T(K) \quad (3)$$

The authors suggest the formation of $Cs_2Mo_2O_7$(g) based on Raman spectra of deposits collected on platinum sheets in the downstream of a transpiration set-up.

We have accounted for Cs_2MoO_4(g) in the description of the gas phase in the present model. However, we have not included $Cs_2Mo_2O_7$(g) at this stage. We recommend to first confirm the formation and stability of such a heavy molecule as $Cs_2Mo_2O_7$(g) (molar weight 569.7 g·mol^{-1}) by analysis directly the gas phase itself using mass spectrometry, and to proceed to the determination of all necessary thermodynamic functions (enthalpy of formation and standard entropy at 298.15 K as well as heat capacity at high temperatures).

3. Thermodynamic model

The optimization was performed using the PARROT module of the Thermo-Calc software (Version 2016b) [54,55]. The Gibbs energy

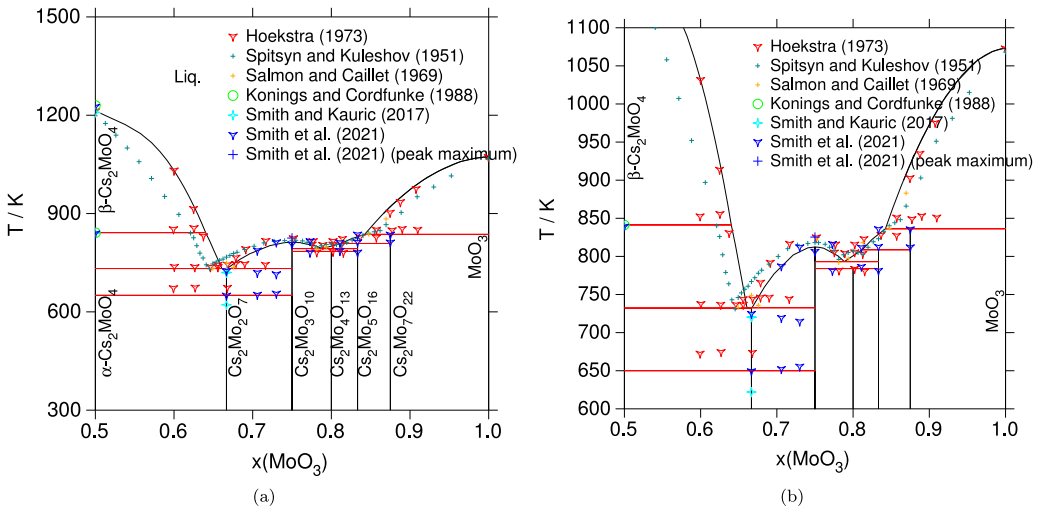

Fig. 2. (a) Pseudo-binary Cs_2MoO_4–MoO_3 phase diagram calculated using the present model compared to the equilibrium data reported in the literature by Spitsyn and Kuleshov [26], Salmon and Caillet [29], Hoekstra [25], and Smith et al. [17]; (b) Enlarged section between $x(MoO_3) = 0.5$ and $x(MoO_3) = 1$ of the pseudo-binary Cs_2MoO_4–MoO_3 phase diagram.

functions in the model are referred to the enthalpy of the pure elements in their stable state at room temperature 298.15 K and 1 bar ($^{o}H_i^{SER}(298.15\,K)$). The optimized parameters are listed in Table 6.

3.1. Pure elements

The Gibbs energy function of the pure element i at temperature T and in its state φ is given by:

$$G_i^{\varphi}(T) - {}^{o}H_i^{SER}(298.15\,K) = a + b\cdot T + c\cdot T\cdot \ln T + \sum d_n T^n \quad (4)$$

where n is an integer $(2, 3, -1 \ldots)$ and a, b, c, and d_n are parameters assessed based on experimental and theoretical information. The parameters reported by Dinsdale are used in this work for pure cesium, molybdenum, and oxygen [56].

3.2. Binary oxides

The binary oxides Cs_7O, Cs_4O, Cs_7O_2, Cs_3O, Cs_2O, CsO, CsO_2, CsO_3, MoO_2, MoO_3, Mo_4O_{11}, Mo_8O_{23}, and Mo_9O_{26} are described as stoichiometric compounds. The corresponding Gibbs energy functions have the same form as in Eq. (4).

$$G^{\varphi}(T) - \sum_i n_i^{\varphi}\,{}^{o}H_i^{SER}(298.15\,K) = a + b\cdot T + c\cdot T\cdot \ln T + \sum d_n T^n \quad (5)$$

where n_i^{φ} is the number of atoms of the element i in the oxide formula. These are taken from the TAF-ID database [14].

3.3. Hexavalent ternary molybdates

Considering the available structural and thermodynamic data in the literature, the present model considers only the existence of the following ternary phases: Cs_2MoO_4 (α and β), $Cs_2Mo_2O_7$ (α and β), $Cs_2Mo_3O_{10}$, $Cs_2Mo_4O_{13}$, $Cs_2Mo_5O_{16}$, and $Cs_2Mo_7O_{22}$. They are treated as stoichiometric. Their Gibbs energies have been expressed based on the recommended enthalpies of formation, entropies and heat capacities (see literature review). The enthalpies of formation and standard entropies have been further optimized to fit the phase equilibrium data in the Cs_2MoO_4–MoO_3 pseudo-binary section. Moreover, only the heat capacity of Cs_2MoO_4 has been optimized, with a single function for the α and β modifications. The heat capacity of $Cs_2Mo_2O_7$ was taken from the selection made in the literature review without further optimization. The heat capacities of $Cs_2Mo_3O_{10}$, $Cs_2Mo_4O_{13}$, $Cs_2Mo_5O_{16}$, and $Cs_2Mo_7O_{22}$ were calculated using the Neumann–Kopp rule applied to Cs_2MoO_4 and MoO_3, and were not further optimized.

The Gibbs energies of the ternary molybdates is given by:

$$G^{\varphi}(T) - \sum_i n_i^{\varphi}\,{}^{o}H_i^{SER}(298.15\,K) = a + b\cdot T + c\cdot T\cdot \ln T + \sum d_n T^n \quad (6)$$

where n_i^{φ} is the number of atoms of the element i in the oxide formula.

3.4. Liquid phase

The liquid phase is described using an ionic two-sublattice model, with Cs^+ and Mo^{4+} cations on the first sublattice, and MoO_4^{2-}, O^{2-} anions, charged vacancies Va^{Q-}, neutral MoO_3, and neutral oxygen O on the second sublattice:

$$(Cs^+, Mo^{4+})_P(MoO_4^{2-}, O^{2-}, Va^{Q-}, MoO_3, O)_Q \quad (7)$$

P and Q are equal to the average charge of the opposite sublattice:

$$Q = y_{Cs^+} + 4y_{Mo^{4+}}$$
$$P = 2y_{MoO_4^{2-}} + 2y_{O^{2-}} + Qy_{Va^{Q-}} \quad (8)$$

where y_i is the site fraction for species i in the sublattice considered. P and Q vary with composition via the site fractions so as to keep the phase electrically neutral.

3.5. Gas phase

The gas phase is described as an ideal mixture of the gaseous species Cs, Cs_2, Cs_2O, Cs_2O_2, CsO, Mo, Mo_2, MoO, MoO_2, MoO_3, Mo_2O_6, Mo_3O_9, Mo_4O_{12}, Mo_5O_{15}, Cs_2MoO_4, O, O_2, and O_3. The Gibbs energy is expressed by:

$$G^{gas} = \sum_i y_i\,{}^{o}G_i^{gas} + RT\sum_i y_i \ln y_i + RT\ln P/P^{o} \quad (9)$$

where y_i is the fraction of the species i in the gas phase, $^{o}G_i^{gas}$ the standard Gibbs energy of the gaseous species i, and P^{o} the standard pressure. The thermodynamic functions of the gaseous species were not optimized in this work. In particular, the Gibbs energy function of Cs_2MoO_4(g) was taken from [51].

4. Results and discussion

4.1. Cs_2MoO_4–MoO_3 pseudo-binary phase diagram

The calculated Cs_2MoO_4–MoO_3 pseudo-binary phase diagram is shown in Figs. 2(a) and 2(b). The associated invariant equilibria are

Table 7
Invariant equilibria calculated in this work compared to the literature data.

Equilibrium reaction	Equilibrium	$x(MoO_3)$	T/K	$\Delta_r H^o_m$/kJ·mol^{-1}	Ref.
α-Cs_2MoO_4 = β-Cs_2MoO_4	Polymorphism	**0.5**	**841.3**	**4.6**	This work
–	–	–	835[a]/839[b] ± 5[a]		[17]
–	–	–	841.3 ± 1.0	(4.6 ± 0.1)	[23,40]
–	–	–	844		[25]
–	–	–	840.2 ± 1.1		[27]
–	–	–	841 ± 1		[57]
β-Cs_2MoO_4 = liq.	Congruent melting	**0.5**	**1223**	**31.8**	This work
–	–	–	1225[a]/1226[b] ± 5[a]		[17]
–	–	–	1229.5 ± 0.2	(31.8 ± 0.8)	[23,41]
–	–	–	1213		[25]
–	–	–	1208.4 ± 0.5		[27]
Liq. = α-Cs_2MoO_4 + β-$Cs_2Mo_2O_7$	Eutectic	**0.661**	**732.2**		This work
–	–	0.645	731		[25,26]
–	–	0.649	733		[29]
α-$Cs_2Mo_2O_7$ = β-$Cs_2Mo_2O_7$	Polymorphism	**0.6667**	**650**	**0.423**	This work
–	–	–	650[a,b] ± 5	(0.423 ± 0.191)[a]	[17]
–	–	–	668		[25]
β-$Cs_2Mo_2O_7$ = Liq.	Congruent melting	**0.667**	**732.5**	**77.7**	This work
–	–	–	725[a,b] ± 5	(81.2 ± 7.1)[a]	[17]
–	–	–	737		[25]
–	–	–	749		[29]
–	–	–	767		[26]
–	–	–	720 ± 1		[27]
Liq. = β-$Cs_2Mo_2O_7$ + $Cs_2Mo_3O_{10}$	Eutectic	**0.6674**	**732.5**		This work
–	–	0.669	736		[25]
–	–	0.676	736		[29]
$Cs_2Mo_3O_{10}$ = Liq.	Congruent melting	**0.75**	**812.3**	**107.9**	This work
–	–	–	806[a,b] ± 5	(81.8 ± 16.8)[a]	[17]
–	–	–	820		[25]
–	–	–	823		[29]
–	–	–	818		[26]
Liq. = $Cs_2Mo_3O_{10}$ + $Cs_2Mo_5O_{16}$	Eutectic	**0.788**	**793.2**		This work
–	–	0.784	798		[25]
–	–	0.781	796		[26]
–	–	0.781	792		[29]
$Cs_2Mo_4O_{13}$ = $Cs_2Mo_3O_{10}$ + $Cs_2Mo_5O_{16}$	Peritectoid	**0.8**	**783.9**		This work
–	–	0.8	776		[25]
–	–	0.8	797		[29]
–	–	0.773(5)	781 ± 10[b]		[17]
–	–	0.811(5)	787 ± 10[b]		[17]
$Cs_2Mo_5O_{16}$ = $Cs_2Mo_7O_{22}$ + Liq.	Peritectic	**0.833**	**808.7**	**134.8**	This work
–	–	–	810[a]/813[b] ± 5	(121.3 ± 8.2)[a]	[17]
–	–	–	823		[25,26]
–	–	0.813	818		[29]
$Cs_2Mo_7O_{22}$ = MoO_3 + Liq	Peritectic	**0.875**	**836.2**	**237.9**	This work
–	–	–	835[a]/836[b] ± 5	(216.5 ± 24.2)[a]	[17]
–	–	0.862	848		[26]
–	–	0.857	846		[25]
–	–	0.847	837		[29]

[a]Data measured by DSC.
[b]Data measured by TG-DSC.

Table 8
Enthalpies of formation and standard entropies of the ternary cesium molybdates optimized in this work.

Compound	$\Delta_f H^o_m$ (298.15 K) (kJ·mol^{-1})		S^o_m (298.15 K) (J·K^{-1}·mol^{-1})	
	Optimized	Selected[a]	Optimized	Selected[a]
α-Cs_2MoO_4	−1517.8	**−(1514.2 ± 4.3)**	247.5	**(248.35 ± 0.30)**
α-$Cs_2Mo_2O_7$	−2302.2	**−(2302.1 ± 8.8)**	315.6	**(317.4 ± 4.3)**
$Cs_2Mo_3O_{10}$	−3060.0	**−(3076.8 ± 16.1)**	414.8	
$Cs_2Mo_4O_{13}$	−3827.6		471.6	
$Cs_2Mo_5O_{16}$	−4585.2	**−(4601.7 ± 37.25)**	541.1	
$Cs_2Mo_7O_{22}$	−6088.4	**−(6087.16 ± 52.16)**	687.0	

[a]Values selected after critical review of the literature (see Section 2).

listed in Table 7. This pseudo-binary system includes three eutectic equilibria, calculated at {$x(MoO_3)$ =0.661 and T = 732.2 K}, {$x(MoO_3)$ =0.6674 and T = 732.5 K}, and {$x(MoO_3)$ =0.788 and T = 793.2 K}, respectively. The transition temperatures (841.3 K for the α to β transition, and 1223 K for the congruent melting) of Cs_2MoO_4 are in very good agreement with the literature data. The α to β transition temperature of $Cs_2Mo_2O_7$ is calculated at 650 K, as reported in the work of Smith et al. [17]. The congruent melting of the same compound is calculated at 732.5 K, in between the data of Smith et al. [17] (i.e. 725 ± 5 K), and the data of Hoekstra [25] (737 K), Salmon and Caillet [29] (749 K), and Spitsyn and Kuleshov [26] (767 K). Note that the nature of the thermal decomposition of β-$Cs_2Mo_2O_7$ (congruent melting or peritectic decomposition) is not known with certitude [17]. In the present model, the calculated congruent melting point is only 0.01 K higher than the eutectic equilibrium {Liq = β-$Cs_2Mo_2O_7$ + $Cs_2Mo_3O_{10}$} and 0.35 K higher than the eutectic equilibrium {Liq = β-$Cs_2Mo_2O_7$ + α-Cs_2MoO_4}, which is not possible to distinguish experimentally. A post-characterization using microscopy would be required after thermal analysis to ascertain if β-$Cs_2Mo_2O_7$ shows a congruent melting or a peritectic decomposition upon heating. The congruent melting of $Cs_2Mo_3O_{10}$ is calculated at 812.3 K, which is again in between the data of Smith et al. [17] (i.e. 806 ± 5 K) and that of Hoekstra [25] (820 K), Salmon and Caillet [29] (823 K), and Spitsyn and Kuleshov [26] (818 K). The calculated peritectoid decomposition of

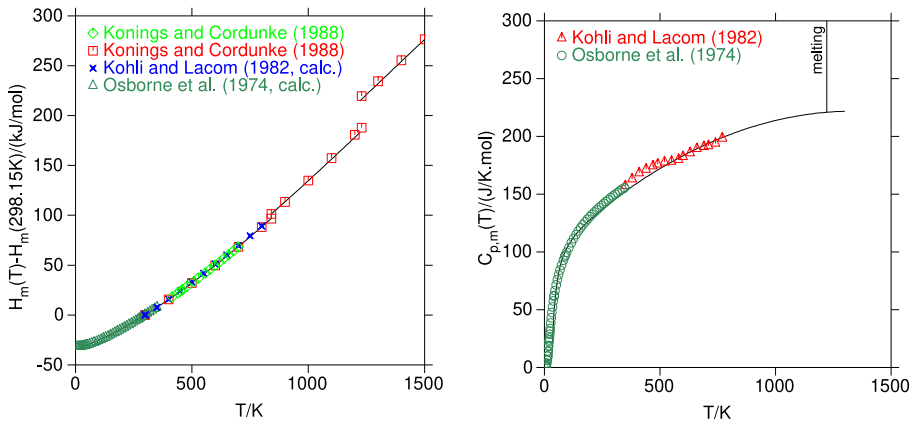

(a) $H^{o}_{m}(T)-H^{o}_{m}(298.15\ K)$ (b) $C^{o}_{p,m}(T)$

Fig. 3. (a) Enthalpy increments of Cs_2MoO_4 calculated with the present description (solid line) compared to the literature data of Osborne et al. [35], Konings and Cordfunke [40], and Kohli and Lacom [42]. (b) Heat capacity of Cs_2MoO_4 calculated with the present description (solid line) compared to the literature data of Osborne et al. [35] and Kohli and Lacom [42].

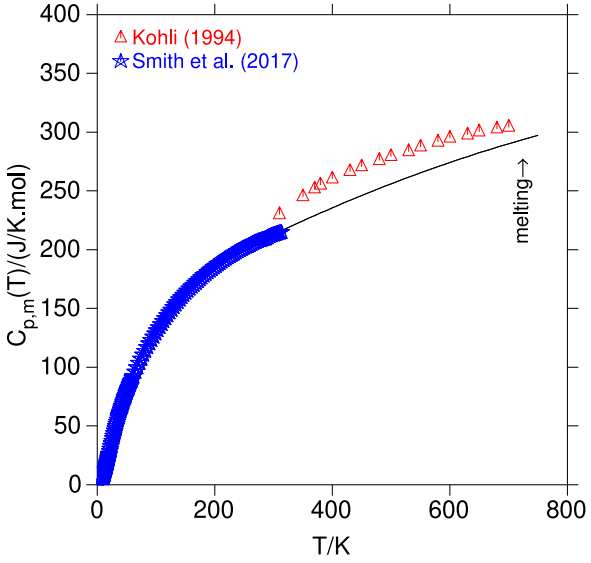

Fig. 4. Heat capacity of $Cs_2Mo_2O_7$ calculated in the model (solid line) compared to the literature data of Kohli [43] and Smith et al. [27].

$Cs_2Mo_4O_{13}$ (783.9 K) is in very good agreement with Smith et al. [17] (781 and 787 K) and Hoekstra [25] (776 K). By contrast with the other studies, Salmon and Caillet report a peritectic decomposition for $Cs_2Mo_4O_{13}$ at 797 K [29], while Spitsyn and Kuleshov [26] report a melting at 807 K. Finally, the calculated peritectic decompositions of $Cs_2Mo_5O_{16}$ and $Cs_2Mo_7O_{22}$ (i.e. 808.7 K and 836.2 K, respectively) are in very good agreement with the data of Smith et al. [17] selected for the optimization.

4.2. Optimized thermodynamic data

The standard enthalpies of formation and standard entropies at 298.15 K optimized in this work are listed in Table 8 and shown in Fig. 5(a), where they are compared to the selected values (see Section 2). A very good agreement is obtained, within the experimental uncertainties.

The calculated enthalpy increments and heat capacities of Cs_2MoO_4 and $Cs_2Mo_2O_7$ are shown in Figs. 3(a), 3(b), and 4, where they are compared to the available literature data. As explained in more detail in the literature review, the estimation by Smith et al. [27] for the heat capacity of $Cs_2Mo_2O_7$ was preferred over the DSC data of Kohli [43]. The heat capacity function at high temperature shows a smooth transition with the low-temperature data.

Finally, the calculated transition enthalpies associated with the invariant reactions in the Cs_2MoO_4–MoO_3 pseudo-binary section are listed in Table 7 and shown in Fig. 5(b), where they are compared to the experimental data available. The enthalpy of fusion of β-Cs_2MoO_4 is in very good agreement with the data of Denielou et al. [41] (selected in the review by Cordfunke and Konings [23]). The calculated transition for the congruent melting of β-$Cs_2Mo_2O_7$ is 77.7 kJ·mol^{-1}, in good agreement with the experimental data within the measured uncertainties. The calculated enthalpy of congruent melting of $Cs_2Mo_3O_{10}$ in the present model is slightly higher than the experimental data,

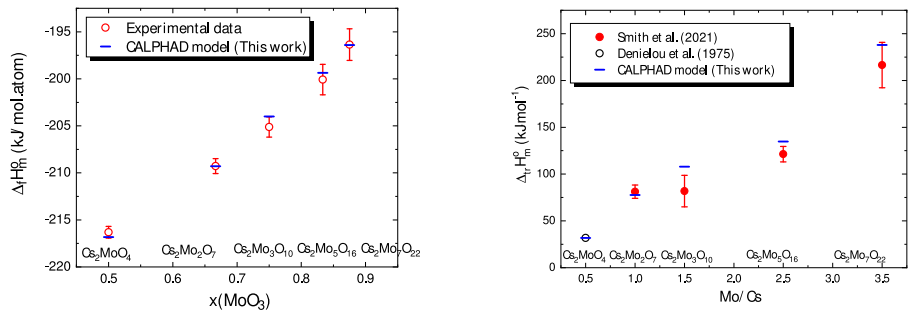

(a) Enthalpy of formation (b) Transition enthalpy

Fig. 5. (a) Enthalpies of formation at 298.15 K calculated in the present model, and comparison with the experimental data selected in this work (see Section 2); (b) Transition enthalpies calculated in the present model at the transition temperature, and comparison with the literature data of Denielou et al. [41] and Smith et al. [17].

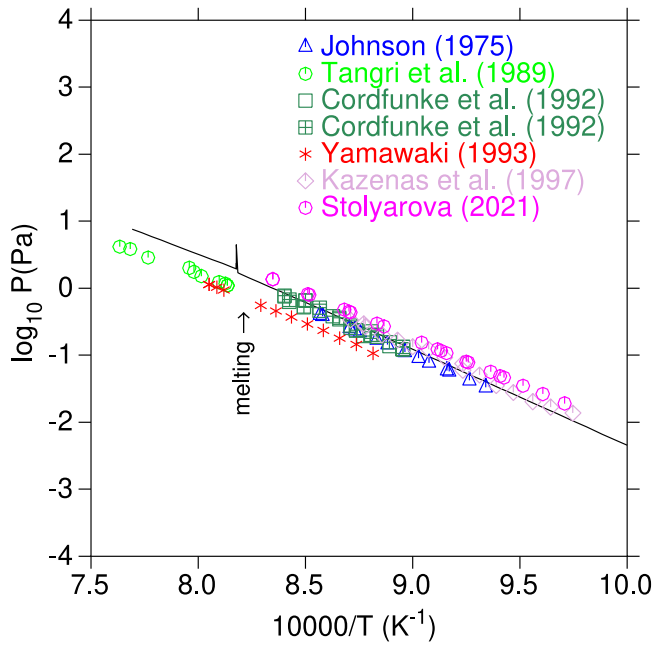

Fig. 6. Calculated total vapour pressure above Cs_2MoO_4(cr) and Cs_2MoO_4(l), and comparison with the data of Johnson [45], Tangri et al. [46], Cordfunke et al. [47], Yamawaki et al. [48], Kazenas et al. [49], and Stolyarova et al. [50].

which might suggest that experimental confirmation is required for these data. The enthalpy of the peritectic decomposition of $Cs_2Mo_5O_{16}$ (134.8 kJ·mol^{-1}) is only slightly higher than the experimental data, i.e. (121.3 ± 8.2) kJ·mol^{-1} [17]. The enthalpy of the peritectic decomposition of $Cs_2Mo_7O_{22}$ (237.9 kJ·mol^{-1}) is in good agreement with the experimental data within the measured uncertainties, i.e. (216.5 ± 24.2) kJ·mol^{-1} [17].

4.3. Vapour pressure above Cs_2MoO_4

The calculated (total) vapour pressure of the congruent equilibrium Cs_2MoO_4(cr, l) = Cs_2MoO_4(g) is shown in Fig. 6 and compared to the data of Johnson [45], Tangri et al. [46], Cordfunke et al. [47], Yamawaki et al. [48], Kazenas et al. [49], and Stolyarova et al. [50]. Note that the thermodynamic functions of Cs_2MoO_4(g) were not optimized in this work, but taken from [51]. Only the thermodynamic functions of Cs_2MoO_4(cr) and of the liquid solution were optimized so as to match as best as possible the known phase diagram data in the Cs_2MoO_4–MoO_3 section and thermodynamic data on Cs_2MoO_4(cr). The calculated vapour pressures are given by the following equations for the temperature ranges 1000–1214 K and 1232–1300 K, respectively:

$$\log_{10} P(Pa) = 11.84 - 14176.1/T(K) \quad (10)$$

$$\log_{10} P(Pa) = 10.21 - 12126.9/T(K) \quad (11)$$

The agreement with the experimental data of Johnson, Cordfunke et al. and Kazenas et al. is generally good, with deviations on the absolute pressures of the order of 19%, 13%, and 10%, respectively. The data of Tangri et al. and Yamawaki et al. are somewhat lower,

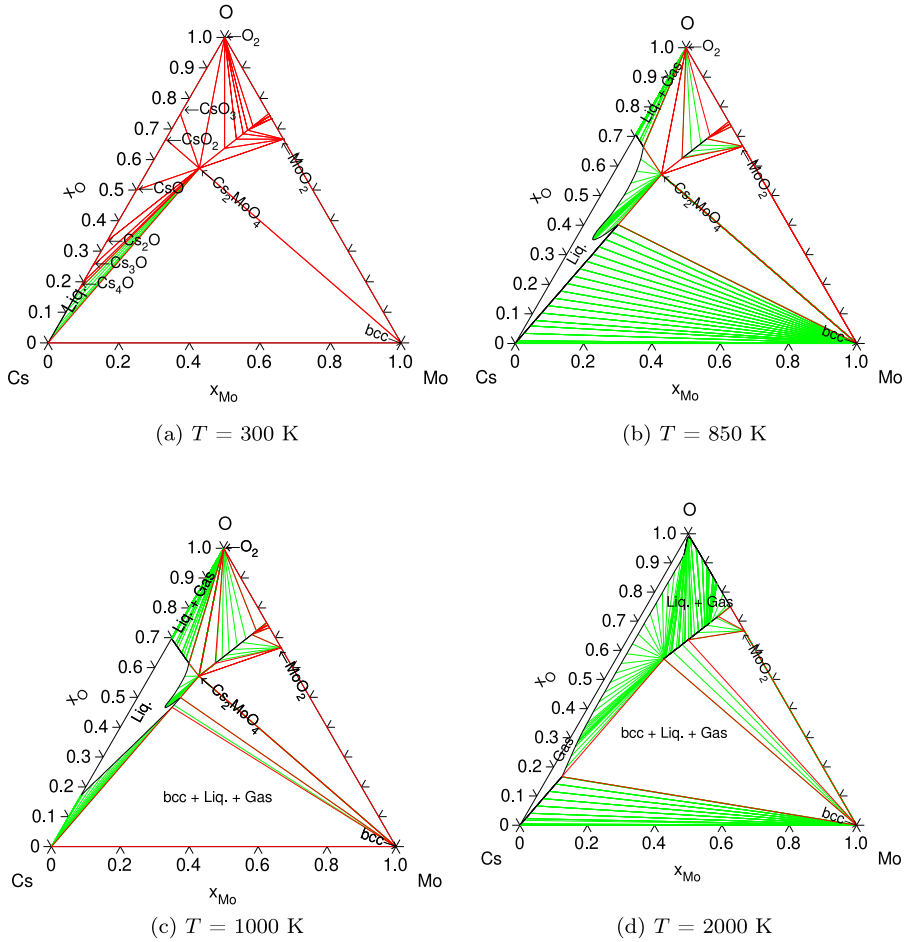

(a) T = 300 K (b) T = 850 K

(c) T = 1000 K (d) T = 2000 K

Fig. 7. Calculated isothermal sections of the Cs–Mo–O system at (a) T = 300 K, (b) T = 850 K, (c) T = 1000 K, and (d) T = 2000 K.

Table A.1
Summary of the thermodynamic data for pure elements and oxides selected in the Cs–Mo system. *SER* refers to the phase of the element stable at 298.15 K.

Phase	Gibbs energy/(J·mol^{-1})	Reference
Liquid		
$(Cs^{+}, Mo^{4+})(Va^{Q-})$	${}^{o}G(Cs^{+})(Va^{Q-})-{}^{o}H^{SER}_{Cs} = G^{Liq}_{Cs}$	[56]
	${}^{o}G(Mo^{4+})(Va^{Q-})-{}^{o}H^{SER}_{Mo} = G^{Liq}_{Mo}$	[56]
	$L^{0}(Cs^{+}, Mo^{4+})_{P}(Va^{Q-})_{Q} = +50000$	[14]
(Cs, Mo) (bcc)		
$(Cs, Mo)(Va)_3$	${}^{o}G(Cs)(Va)_3-{}^{o}H^{SER}_{Cs} = G^{SER}_{Cs}$	[56]
	${}^{o}G(Mo)(Va)_3-{}^{o}H^{SER}_{Mo} = G^{SER}_{Mo}$	[56]
	$L^{0}(Cs, Mo)(Va)_3 = +50000$	[14]
Gas		
(Cs, Cs_2, Mo, Mo_2)	${}^{o}G^{gas}_{Cs} - {}^{o}H^{SER}_{Cs} = G^{G}_{Cs} + RTln\ (10^{-5}P)$	[58]
	${}^{o}G^{gas}_{Cs_2} - 2{}^{o}H^{SER}_{Cs} = G^{G}_{Cs_2} + RTln\ (10^{-5}P)$	[58]
	${}^{o}G^{gas}_{Mo} - {}^{o}H^{SER}_{Mo} = G^{G}_{Mo} + RTln\ (10^{-5}P)$	[56]
	${}^{o}G^{gas}_{Mo_2} - 2{}^{o}H^{SER}_{Mo} = G^{G}_{Mo_2} + RTln\ (10^{-5}P)$ [56]	
Functions	$G^{SER}_{Cs} = -17373.82 + 436.899787T - 90.5212584Tln\ (T)+0.2029422T^2$	[56]
	$- 1.27907669\cdot10^{-4}T^3 + 245245T^{-1}$ (298 < T/K < 301.59 K)	
	$= -13553.817+218.689955T - 46.7273304Tln\ (T) + 0.02043269T^2$	
	$- 4.074846\cdot10^{-6}T^3+181528T^{-1}+7.8016\cdot10^{21}T^{-9}$ (301.59<T/K<2000 K)	
	$G^{SER}_{Mo} = -7746.302 + 131.9197T - 23.56414Tln\ (T) - 0.003443396T^2$	[56]
	$+ 5.66283\cdot10^{-7}T^3 + 65812T^{-1} - 1.30927\cdot10^{-10}T^4$ (298 < T/K < 2896 K)	
	$G^{Liq}_{Cs} = -15282.679 + 429.968752T - 90.5212584Tln\ (T) + 0.2029422T^2$	[56]
	$- 1.27907669\cdot10^{-4}T^3 + 245245T^{-1} - 3.56867\cdot10^{-18}T^7$ (298 < T/K < 301.59 K)	
	$= -11454.038 + 211.728844T - 46.7273304Tln\ (T)+0.02043269T^2$	
	$- 4.074846\cdot10^{-6}T^3+181528T^{-1}$ (301.59 < T/K < 2000 K)	
	$G^{Liq}_{Mo} = +34085.045+117.224788T - 23.56414Tln\ (T)$	[56]
	$- 0.003443396T^2+5.66283\cdot10^{-7}T^3 + 65812T^{-1} - 1.30927\cdot10^{-10}T^4$	
	$+ 4.24519\cdot10^{-22}T^7$ (298 < T < 2896 K)	
	$= +3538.963 + 271.6697T - 42.63829Tln\ (T)$ (2896 < T < 5000 K)	

Table A.2
Summary of the thermodynamic data for pure elements and oxides selected in the Cs–Mo system. *SER* refers to the phase of the element stable at 298.15 K.

Phase	Gibbs energy/(J·mol^{-1})	Reference
Functions	$G^{G}_{Cs} = +70221.1857 - 34.9432617T - 21.01225Tln\ (T)$	[58]
	$+ 2.3869595\cdot10^{-4}T^2 - 4.17045667\cdot10^{-8}T^3 + 4922.448T^{-1}$ (298 < T < 1600 K)	
	$= +65030.9624+16.0373197T - 28.23664Tln\ (T)$	
	$+ 0.0041988735T^2 - 4.22771\cdot10^{-7}T^3 + 522968.5T^{-1}$ (1600 < T < 3400 K)	
	$= +366608.608 - 1031.64395T + 100.1023Tln\ (T)$	
	$- 0.020285495T^2 + 4.61329\cdot10^{-7}T^3 - 1.333813\cdot10^{8}T^{-1}$ (3400 < T < 5300 K)	
	$= +21277.4247 - 330.32731T + 20.43107ln\ (T) - 0.012545005T^2$	
	$+ 3.32779833\cdot10^{-7}T^3 + 1.375229\cdot10^{8}T^{-1}$ (5300 < T < 7000 K)	
	$= -1347367.73 + 2313.0949T - 278.8398Tln\ (T) + 0.016571635T^2$	
	$- 1.98924\cdot10^{-7}T^3 + 1.3125275\cdot10^{9}T^{-1}$ (7000 < T < 100000 K)	
	$G^{G}_{Cs_2} = +100114.046 - 81.8752338T - 29.1921Tln\ (T)$	[58]
	$- 0.01584241T^2+4.411035\cdot10^{-6}T^3 - 87527.95T^{-1}$ (298<T<700 K)	
	$= +76365.6162+232.868668T - 76.74226Tln\ (T)+0.026454175T^2$	
	$- 2.64218333\cdot10^{-6}T^3 + 2135020T^{-1}$ (700 < T < 1700 K)	
	$= +250375.533 - 857.020867T + 68.80663Tln\ (T) - 0.028077265T^2$	
	$+ 1.22328533\cdot10^{-6}T^3 - 37126965T^{-1}$ (1700<T<3000 K)	
	$= -161131.901 + 641.492817T - 115.7658Tln\ (T)+0.008419445T^2$	
	$- 1.1690215\cdot10^{-7}T^3 + 1.3370865\cdot10^{8}T^{-1}$ (3000 < T < 4900 K)	
	$= -155428.026 + 692.773744T - 122.889Tln\ (T)+0.01069752T^2$	
	$- 2.11018\cdot10^{-7}T^3 + 1.1397085\cdot10^{8}T^{-1}$ (4900 < T < 6000 K)	
	$G^{G}_{Mo} = +651326.983 - 41.0946081T - 21.0437Tln\ (T)$	[59]
	$+ 2.7252545\cdot10^{-4}T^2 - 4.77857833\cdot10^{-8}T^3 + 5594.93T^{-1}$ (298 < T < 1600 K)	
	$= +633752.125+83.3186552T - 37.98605Tln\ (T) + 0.007623775T^2$	
	$-6.52545667\cdot10-7T^3 + 3471277.5T^{-1}$ (1600 < T < 3500 K)	
	$= +1134689.66 - 1617.69443T + 169.6658Tln\ (T) - 0.03080567T^2$	
	$+ 6.87557667\cdot10^{-7}T^3 - 2.240338\cdot10^{8}T^{-1}$ (3500 < T < 5000 K)	
	$= +1008188.16 - 1437.30781T + 150.7395Tln\ (T) - 0.03086233T^2$	
	$+ 7.54569333\cdot10^{-7}T^3 - 1.0601775\cdot10^{8}T^{-1}$ (5000 < T < 6200 K)	
	$G^{G}_{Mo_2} = +892320.138 + 5.95304372T - 37.156Tln\ (T)$	[59]
	$+ 3.61\cdot10^{-5}T^2 - 1.10858333\cdot10^{-7}T^3 + 113615T^{-1}$ (298 < T < 1000 K)	
	$= +878307.025+162.383892T - 60.077Tln\ (T)$	
	$+ 0.0165846T^2 - 2.3378\cdot10^{-6}T^3 + 1706980T^{-1}$ (1000 < T < 1800 K)	
	$= +1105100.83 - 1223.34666T + 124.219Tln\ (T) - 0.05020415T^2$	
	$+ 2.21706167\cdot10^{-6}T^3 - 50788800T^{-1}$ (1800 < T < 3100 K)	
	$= +641365.422+619.744903T - 105.798Tln\ (T)$	
	$+ 6.5385\cdot10^{-4}T^2 + 1.02916667\cdot10^{-7}T^3 + 1.25079\cdot10^{8}T^{-1}$ (3100 < T < 6000 K)	

with deviations of the order of 51% and 53%–59%, respectively, while the data of Stolyarova et al. is higher than calculated in the model with deviations of the order of 45%. Cordfunke et al. [47] mention that the lower vapour pressure results of Tangri et al. above Cs_2MoO_4(l) might come from the use of an alumina condenser tube and the reaction of Cs_2MoO_4(g) with alumina at high temperatures. The same might be

true for the measurements of Yamawaki et al. Thus the latter two sets of data could be less reliable. The origin of the slightly higher vapour pressures measured by Stolyarova et al. compared to the studies of Johnson, Cordfunke et al. and Kazenas et al. is unclear. Complementary measurements above liquid cesium molybdate would be valuable to compare with the present calculation.

4.4. Calculated Cs–Mo–O isotherms

Finally, isotherms are calculated at relevant temperatures for the safety assessment of the oxide fuel pin behaviour in a fast neutron reactor, i.e. at $T = 300$ K, $T = 850$ K, $T = 1000$ K and $T = 2000$ K. They are shown in Figs. 7(a)–7(c), and 7(d), respectively. Note that under "standard" irradiation conditions, such as in the Phénix sodium-cooled fast reactor, the expected temperatures at the pellet rim and centre range between 700 and 2400 K, respectively, as reported by Samuelsson et al. [10]. 850 K was selected as a representative temperature for the JOG layer, while 1000 K is a temperature that can be expected on the surface of the JOG layer on the fuel side. 2000 K was selected for the calculation as representative temperature for the centre of the fuel pin. In the JOG layer, the main constituent, i.e. Cs_2MoO_4, is thus expected in its hexagonal β modification. In regions of the fuel pin where the temperature is higher than 1223 K, the presence of the cesium molybdate can lead to the formation of a liquid phase.

5. Conclusions

This work reports a thermodynamic modelling assessment of the key fission product system Cs–Mo–O, using formalisms compatible with the TAF-ID database, namely the compound energy formalism and ionic-two sublattice model. The overall agreement with the available experimental data on thermodynamic properties and vapour pressure of ternary cesium polymolybdates, and phase diagram equilibria in the Cs_2MoO_4–MoO_3 pseudo-binary section is generally good. A few issues remain unresolved still, that would benefit from complementary investigations:

- The polymorphism of $Cs_2Mo_4O_{13}$ needs further investigations to determine the nature and exact temperature of the phase transition between the reported triclinic (in space group $P-1$) and monoclinic (in space group $C2/c$) modifications.
- To determine the exact nature of the thermal decomposition of β-$Cs_2Mo_2O_7$, i.e. congruent melting or peritectic decomposition, post microscopic characterizations would be necessary after thermal analysis measurements.
- The low-temperature heat capacities and standard entropies at 298.15 K of $Cs_2Mo_3O_{10}$, $Cs_2Mo_4O_{13}$, $Cs_2Mo_5O_{16}$, $Cs_2Mo_7O_{22}$, as well as standard enthalpy of formation at 298.15 K of $Cs_2Mo_4O_{13}$ have not been measured to this date.
- The high temperature heat capacities (and/or enthalpy increments) of $Cs_2Mo_2O_7$, $Cs_2Mo_3O_{10}$, $Cs_2Mo_4O_{13}$, $Cs_2Mo_5O_{16}$, $Cs_2Mo_7O_{22}$ should be determined experimentally.
- We recommend to confirm the congruent vaporization of $Cs_2Mo_2O_7$ as suggested by Do et al. [52] using mass spectrometry before introducing $Cs_2Mo_2O_7$(g) gaseous species in the thermodynamic model of the Cs–Mo–O system. The current data available are derived from the thermogravimetry method, which gives only the total vapour pressure. Using a technique such as Knudsen Effusion Mass Spectrometry would allow to obtain more reliable results. The thermodynamic functions of $Cs_2Mo_2O_7$(g) would then need to be determined too.
- The vapour pressure above liquid Cs_2MoO_4 should be scrutinized again with complementary measurements using a technique such as transpiration or Knudsen effusion Mass Spectrometry.

Declaration of competing interest

The authors declare that they have no known competing financial interests or personal relationships that could have appeared to influence the work reported in this paper.

Data availability statement

The data presented herein are available from the corresponding author upon request.

Acknowledgement

Modelling of the Cs–Mo–O system was supported by the OECD/NEA TAF-ID (Thermodynamics of Advanced Fuels – International Database) project.

Appendix. Thermodynamic modelling assessment of the Cs–Mo system

See Tables A.1 and A.2.

References

[1] H. Kleykamp, The chemical state of the fission products in oxide fuels, J. Nucl. Mater. 131 (1985) 221–246.
[2] Y. Guerin, Fuel performance of fast spectrum oxide fuel, in: Comprehensive Nuclear Materials, Elsevier, 2012 (Chapter 2.21).
[3] J. Rest, A.W. Cronenberg, Modeling the behavior of Xe, I, Cs, Te, Ba and Sr in solid and liquefied fuel during severe accidents, J. Nucl. Mater. 150 (1987) 203–225.
[4] F. Cappia, B.D. Miller, J.A. Aguiar, L. He, D.J. Murray, B.J. Frickey, J.D. Stanek, J.M. Harp, Electron microscopy characterization of fast reactor MOX joint oxyde-gaine (JOG), J. Nucl. Mater. 531 (2020) 151964.
[5] M. Tourasse, M. Boidron, B. Pasquet, Fission product behaviour in Phenix fuel pins at high burn-up, J. Nucl. Mater. 1800 (1992) 49–57.
[6] J.-C. Dumas, Etude des Conditions de Formation Du Joint-Oxyde-Gaine Dans Les Combustibles Oxydes Mixtes des Reacteurs à Neutrons Rapides, Observations et Proposition D'Un Modèle de Comportement des Produits de Fission Volatils (Ph.D. thesis), Institut national polytechnique de Grenoble, Grenoble, France, 1995.
[7] K. Maeda, T. Asaga, Change of fuel-to-cladding gap width with the burn-up in FBR MOX fuel irradiated to high burn-up, J. Nucl. Mater. 327 (2004) 1–10.
[8] T.N.P. Thi, Caractérisation et Modélisation Du Comportement Thermodynamique Du Combustible RNR-Na Sous Irradiation (Ph.D. thesis), Ecole Doctorale Physique et Sciences de la Matière, Aix-Marseille University, 2014.
[9] R. Parrish, A. Winston, J. Harp, A. Aitkaliyeva, TEM characterization of high burnup fast-reactor MOX fuel, J. Nucl. Mater. 527 (2019) 151794.
[10] K. Samuelsson, J.-C. Dumas, B. Sundman, J. Lamontagne, C. Guéneau, Simulation of the chemical state of high burnup (U,Pu)O2 fuel in fast reactors based on thermodynamic calculations, J. Nucl. Mater. 532 (2020) 151969.
[11] T. Ishii, T. Mizuno, Thermal conductivity of cesium molybdate Cs2MoO4, J. Nucl. Mater. 231 (1996) 242–244.
[12] K. Minato, M. Takano, K. Fukuda, S. Sato, H. Ohashi, Thermal expansion and thermal conductivity of cesium molybdate, J. Nucl. Mater. 255 (1997) 18–23.
[13] G. Wallez, P.E. Raison, A.L. Smith, N. Clavier, N. Dacheux, J. Solid State Chem. 215 (2014) 225–230.
[14] C. Guéneau, N. Dupin, L. Kjellqvist, E. Geiger, M. Kurata, S. Gossé, E. Corcoran, A. Quaini, R. Hania, A.L. Smith, M.H.A. Piro, T. Besmann, P.E.A. Turchi, J.C. Dumas, M.J. Welland, T. Ogata, B.O. Lee, J.R. Kennedy, C. Adkins, M. Bankhead, D. Costa, TAF-ID: An international thermodynamic database for nuclear fuel applications, CALPHAD 72 (2021) 102212.
[15] P. Villars, K. Cenzual, Pearson's Crystal Data - Crystal Structure Database for Inorganic Compounds, Release 2018/2019, ASM International, Materials Park, Ohio, USA, 2018/2019.
[16] O. Fabrichnaya, Cesium-molybdenum-oxygen, in: Ternary Alloy Systems: Phase Diagrams, Crystallographic and Thermodynamic Data Critically Evaluaed By MSIT, Subvol. C. Non-Ferrous Metal Systems. Pt. 4: Selected Nuclear Materails and Engineering Systems, Springer-Verlag, Berlin-Heidelberg, Germany, 2007, pp. 244–259.
[17] A.L. Smith, J. Vlieland, M.-C. Pignié, M. Abbink, G. Mikaelian, P. Benigni, New insights into the Cs-Mo-O system: Experimental studies of the Cs2MoO4-MoO3 pseudo-binary system, Thermochim. Acta 696 (2021) 178825.
[18] C. Guéneau, J.-L. Flèche, Thermodynamic assessment of the cesium-oxygen system by coupling density functinoal theory and CALPHAD approaches, CALPHAD 49 (2015) 67–78.

[19] E.C. Corcoran, J.-L. Flèche, N. Dupin, B. Sundman, C. Guéneau, Thermodynamic investigations of the uranium-molybdenum-oxygen system by a coupling of density functional theory and CALPHAD methodologies, CALPHAD 63 (2018) 196–211.

[20] G. Kauric, Etude de l'Interaction Entre Le Combustible MOX et Le Sodium Pour la SuretÉ des RÉacteurs à Neutrons Rapides à Caloporteur Sodium (RNR), Study of the Nuclear Fuel-Sodium Coolant Interaction for the Safety Assessment of Sodium-Cooled Fast Reactors (Ph.D. thesis), University Paris-Saclay, France, 2020.

[21] A.L. Smith, M. Rutten, L. Herrmann, E. Epifano, R.J.M. Konings, E. Colineau, J.-C. Griveau, C. Guéneau, N. Dupin, Experimental studies and thermodynamic assessment of the Ba-Mo-O system by the CALPHAD method, J. Eur. Ceram. Soc. 41 (2021) 3664–3686.

[22] C. Guéneau, S. Gosse, A. Quani, N. Dupin, B. Sundman, M. Kurata, T. Besmann, P. Turchi, J.-C. Dumas, E.-C. Corcoran, et al., FUELBASE, TAF-ID databases and OC software. Advanced computational tools to perform thermodynamic calculations on nuclear fuel materials, in: The 7^{th} European Review Meeting on Severe Accident Research, ERMSAR-2015, 24-26 March 2015, Marseille, France, 2015.

[23] E.H.P. Cordfunke, R.J.M. Konings, Thermochemical Data for Reactor Materials and Fission Products, Elsevier Science Publishers B. V., Amsterdam, North-Holland, 1990.

[24] A.S. Pakhomova, D.V. Spiridonova, S.V. Krivovichev, Crystal structure of β-Cs2Mo4O13, Radiochemistry 53 (2011) 358–360.

[25] H.R. Hoekstra, Cs2MoO4-MoO3 system, Inorg. Nucl. Chem. Lett. 9 (1973) 1291–1301.

[26] V.I. Spitsyn, I.M. Kuleshov, J. Gen. Chem. USSR 21 (1951) 1493.

[27] A.L. Smith, G. Kauric, L. van Eijck, K. Goubitz, G. Wallez, J.-C. Griveau, E. Colineau, N. Clavier, R.J.M. Konings, Structural and thermodynamic study of dicesium molybdate Cs2Mo2O7: Implications for fast neutron reactors, J. Solid State Chem. 253 (2017) 89–102.

[28] J. Marrot, J.M. Savariault, Acta Crystallogr. C 51 (1995) 2201–2205.

[29] R. Salmon, P. Caillet, Polymolybdates et polytungstates de rubidium ou de cesium anhydres, Bull. Soc. Chim. Fr. 5 (1969) 1569–1573.

[30] Zh.G. Bazarova, K.N. Fedorov, M.V. Mokhosoev, R.P. Shulunov, G.D. Tsyrenova, L.N. Korsun, A physicochemical study of the Cs2MoO4-MoO3 system, Russ. J. Inorg. Chem. 35 (1990) 1505–1508.

[31] P.A.G. O'Hare, H.R. Hoekstra, Thermochemistry of molybdates. I. standard enthalpy of formation of cesium molybdate (Cs2MoO4), J. Chem. Thermodyn. 5 (1973) 851–856.

[32] P.A.G. O'Hare, H.R. Hoekstra, Thermochemistry of molybdates V. Standard enthaly of formation of cesium dimolybdate, J. Chem. Thermodyn. 7 (1975) 279–284.

[33] A.L. Smith, M.-C. Pignié, L. van Eijck, J.-C. Griveau, E. Colineau, R.J.M. Konings, Thermodynamic study of Cs3Na(MoO4)2: Determination of the standard enthalpy of formation and standard entropy at 298.15 K, J. Chem. Thermodyn. 120 (2018) 205–216.

[34] P. Benigni, G. Mikaelian, E. Ruiz, C. Perrin-Pellegrino, J. Rogez, Calorimetric determination of the formation enthalpies of Cs polymolybdates at 298.15 K and 0.1 MPa, J. Chem. Eng. Data 65 (8) (2020) 3875–3883.

[35] D.W. Osborne, H.E. Flotow, H.R. Hoekstra, Cesium molybdate, Cs2MoO4: Heat capacity and thermodynamic properties from 5 to 350 K, J. Chem. Thermodyn. 6 (2) (1974) 179–183.

[36] B.A. Staskiewicz, J.R. Tucker, P.E. Snyder, The heat of formation of molybdenum dioxide and molybdenum trioxide, J. Am. Chem. Soc. 77 (11) (1955) 2987–2989.

[37] A.D. Mah, Heats of formation of alumina, molybdenum trioxide and molybdenum dioxide, J. Phys. Chem. 61 (11) (1957) 1572–1573.

[38] R. Guillaumont, T. Fanghänel, J. Fuger, I. Grenthe, V. Neck, D.A. Palmer, M.H. Rand, Update on the Chemical Thermodynamics of Uranium, Neptunium, Plutonium, Americium & Technetium, OECD Nuclear Energy Agency, Data Bank, Issy-les-Moulineaux, France, 2003.

[39] D.R. Fredrickson, M.G. Chasanov, Anal. Calorim. (1974) 723–730.

[40] R.J.M. Konings, E.H.P. Cordfunke, The thermochemical properties of cesium molybdate, Cs2MoO4, from 298.15 to 1500 K, Thermochim. Acta 124 (1988) 157–162.

[41] L. Denielou, J.P. Petitet, C. Tequi, High temperature calorimetric measurements: Silver sulphate and alkali chromates, molybdates, and tungstates, J. Chem. Thermodyn. 7 (1975) 901–902.

[42] R. Kohli, W. Lacom, Heat capacity and thermodynamic properties of the alkali metal compounds in the temperature range 300-800 K. I. Cesium and rubidium molybdates, Thermochim. Acta 57 (1982) 155–160.

[43] R. Kohli, Heat capacty and thermodynamic properties of alkali metal compounds. Part 7. Cesium and rubidium dimolybdates, Thermochim. Acta 237 (1994) 241–245.

[44] D.F. Smith, D. Brown, A.S. Dworkin, D.J. Sasmor, E.R. Artsdalen, J. Am. Chem. Soc. 78 (8) (1956) 1533–1536.

[45] I. Johnson, Mass spectrometric study of the vaporization of cesium and sodium molybdates, J. Phys. Chem. 79 (1975) 722–726.

[46] R.P. Tangri, V. Venugopal, D.K. Bose, M. Sundaresan, Thermodynamics of vaporisation of caesium mmolybdate, J. Nucl. Mater. 167 (1989) 127–130.

[47] E.H.P. Cordfunke, R.J.M. Konings, S.R.M. Meyssen, Vapour pressures of some caesium compounds II. Cs2MoO4 and Cs2RuO4, J. Chem. Thermodyn. 24 (1992) 725–728.

[48] M. Yamawaki, T. Oka, M. Yasumoto, H. Sakurai, Thermodynamics of vaporization of cesium molybdate by means of mass spectrometry, J. Nucl. Mater. 201 (1993) 257–260.

[49] E.K. Kazenas, I.O. Samoilova, G.K. Astakjova, Mass-spectrometric investigation of the sublimation of cesium molybdate, Russ. Metall. 4 (1997) 39–42.

[50] V.L. Stolyarova, V.A. Vorozhtcov, S.I. Lopatin, S.M. Shugurov, E.P. Simonenko, N.O. Simonenko, K. Masaki, D. Costa, Vaporization and thermodynamics of the Cs2O–MoO3 system studied using high-temperature mass spectrometry, Rapid. Commun. Mass Spectrom. 35 (12) (2021) e9097.

[51] C.W. Bale, P. Chartrand, S.A. Degterov, G. Eriksson, K. Hack, R. Ben Mahfoud, J. Melançon, A.D. Pelton, S. Petersen, FactSage thermochemical softwares and databases, CALPHAD 26 (2) (2002) 189–228.

[52] T.-M.-D. Do, S. Sujatanond, Y. Tachibana, T. Ogawa, J. Nucl. Sci. Technol. 54 (2017) 330–336.

[53] D.M. Price, Vapor pressure determination by thermogravimetry, Thermochim. Acta 367–368 (2001) 253–262.

[54] B. Jansson, Report TRITA-MAC-0234, Royal Institute Technology, S10044 Stockholm 70, Sweden, 1984.

[55] B. Sundman, B. Jansson, J.O. Andersson, The thermo-calc databank system, CALPHAD 9 (1985) 153–190.

[56] A. Dinsdale, SGTE data for pure elements, CALPHAD 15 (1991) 317–425.

[57] Z.A. Solodovnikova, S.F. Solodovnikov, E.S. Zolotova, New triple molybdates Cs3LiCo2(MoO4)4 and Rb3LiZn2(MoO4)4, filled derivatives of the cs6zn5(moo4)8 type, Acta Crystallogr. C 62 (2006) 16–18.

[58] V.P. Glushko, L.V. Gurvich, I.V. Weitz, V.A. Medvedev, G.A. Hachkuruzov, V.S. Jungmann, G.A. Bergman, V.F. Baibuz, V.S. Iorish, et al., Thermodynamic Properties of Individual Substances, vol. 2, Book 2, 1979.

[59] I. Ansara, B. Sundman, Scientific Group Thermodata Europe, Computer Handling and Determination of Data, North Holland, Amsterdam, 1986,